Marine and Petroleum Geology 26 (2009) 1483–1498

Contents lists available at ScienceDirect

Marine and Petroleum Geology

journal homepage: www.elsevier.com/locate/marpetgeo

Gas hydrates in the western deep-water Ulleung Basin, East Sea of Korea

Byong-Jae Ryu [a,*], Michael Riedel [b], Ji-Hoon Kim [a], Roy D. Hyndman [c], Young-Joo Lee [a], Bu-Heung Chung [a], Il-Soo Kim [d]

[a] Petroleum and Marine Resources Research Division, Korea Institute of Geoscience and Mineral Resources, 92 Gwahang-no, Yuseong-gu, Daejeon 305-350, Republic of Korea
[b] Department of Earth and Planetary Sciences, McGill University, Montreal, QC H3A 2A7, Canada
[c] Pacific Geoscience Centre, Geological Survey of Canada, 9860 W. Saanich Rd., Sidney, B.C. V8L 4B2, Canada
[d] Overseas Office, Korea National Oil Corporation, 1588-14 Gwanyang-dong, Dongan-gu, Anyang-si, Gyeonggi-do 431-711, Republic of Korea

ARTICLE INFO

Article history:
Received 14 May 2008
Received in revised form
13 February 2009
Accepted 17 February 2009
Available online 27 February 2009

Keywords:
Gas hydrate
Ulleung Basin
Total organic carbon
Bottom-simulating reflector
Seismic blanking zone

ABSTRACT

Geophysical surveys and geological studies of gas hydrates in the western deep-water Ulleung Basin of the East Sea off the east coast of Korea have been carried out by the Korea Institute of Geoscience and Mineral Resources (KIGAM) since 2000. The work included a grid of 4782 km of 2D multi-channel seismic reflection lines and 11 piston cores 5–8 m long. In the piston cores, cracks generally parallel to bedding suggest significant in-situ gas. The cores showed high amounts of total organic carbon (TOC), and from the southern study area showed high residual hydrocarbon gas concentrations. The lack of higher hydrocarbons and the carbon isotope ratios indicate that the methane is primarily biogenic. The seismic data show areas of bottom-simulating reflectors (BSRs) that are associated with gas hydrates and underlying free gas. An important observation is the numerous seismic blanking zones up to 2 km across that probably reflect widespread fluid and gas venting and that are inferred to contain substantial gas hydrate. Some of the important results are: (1) BSRs are widespread, although most have low amplitudes; (2) increased P-wave velocities above some BSRs suggest distributed low to moderate concentration gas hydrate whereas a velocity decrease below the BSR suggests free gas; (3) the blanking zones are often associated with upbowing of sedimentary bedding reflectors in time sections that has been interpreted at least in part due to velocity pull-up produced by high-velocity gas hydrate. High gas hydrate concentrations are also inferred in several examples where high interval velocities are resolved within the blanking zones. Recently, gas hydrate recoveries by the piston coring and deep-drilling in 2007 support the interpretation of substantial gas hydrate in many of these structures.

1. Introduction

This article reports geophysical and geological surveys, and related studies of marine gas hydrates in the East Sea, off the east coast of Korea. Because gas hydrate contains a large amount of organic carbon and widely occurs in deep oceans and permafrost regions, it is of interest as a potential energy resource in the future (e.g., Kvenvolden, 1993), as well as a possible source of atmospheric methane affecting global climate and contributing to global warming (e.g., MacDonald, 1990; Haq, 2000). Gas hydrate may also constitute a natural hazard in situations where rapid dissociation triggers submarine landslides and associated tsunamis (e.g., McIver, 1982; Paull et al., 2000a).

Significant geophysical exploration and study of the Ulleung Basin of the East Sea (Fig. 1) began as conventional oil and gas exploration on its southern continental shelf in the late 1960s. Since the early 1990s, there have been extensive research surveys in the deep-water area by the Korea Institute of Geoscience and Mineral Resources (KIGAM) and the Korea Ocean Research and Development Institute (KORDI). These surveys and studies were mainly focused on the tectonic history, sediment stratigraphy and paleoenvironment of the East Sea. Gardner et al. (1998) reported an initial reconnaissance study of marine gas hydrates in the Ulleung Basin mainly using 12 kHz MR1 sidescan sonar images, core samples, and 3.5 kHz sub-bottom profiling records.

A preliminary study of geophysical indicators of gas hydrate in the southwestern part of the Ulleung Basin using multi-channel reflection seismic data was reported by Lee et al. (2005). Horozal et al. (2008) provided a regional geological and thermal interpretation. The presence of substantial gas hydrates in the blank zone structures has recently been confirmed by the piston coring and a deep-drilling expedition in 2007 for which there are initial reports (NETL, 2007; Park, 2008; Park et al., 2008; Kim et al., 2008).

* Corresponding author. Tel.: +82 42 868 3211; fax: +82 42 868 3417.
E-mail address: bjryu@kigam.re.kr (B.-J. Ryu).

0264-8172/$ – see front matter © 2009 Elsevier Ltd. All rights reserved.
doi:10.1016/j.marpetgeo.2009.02.004

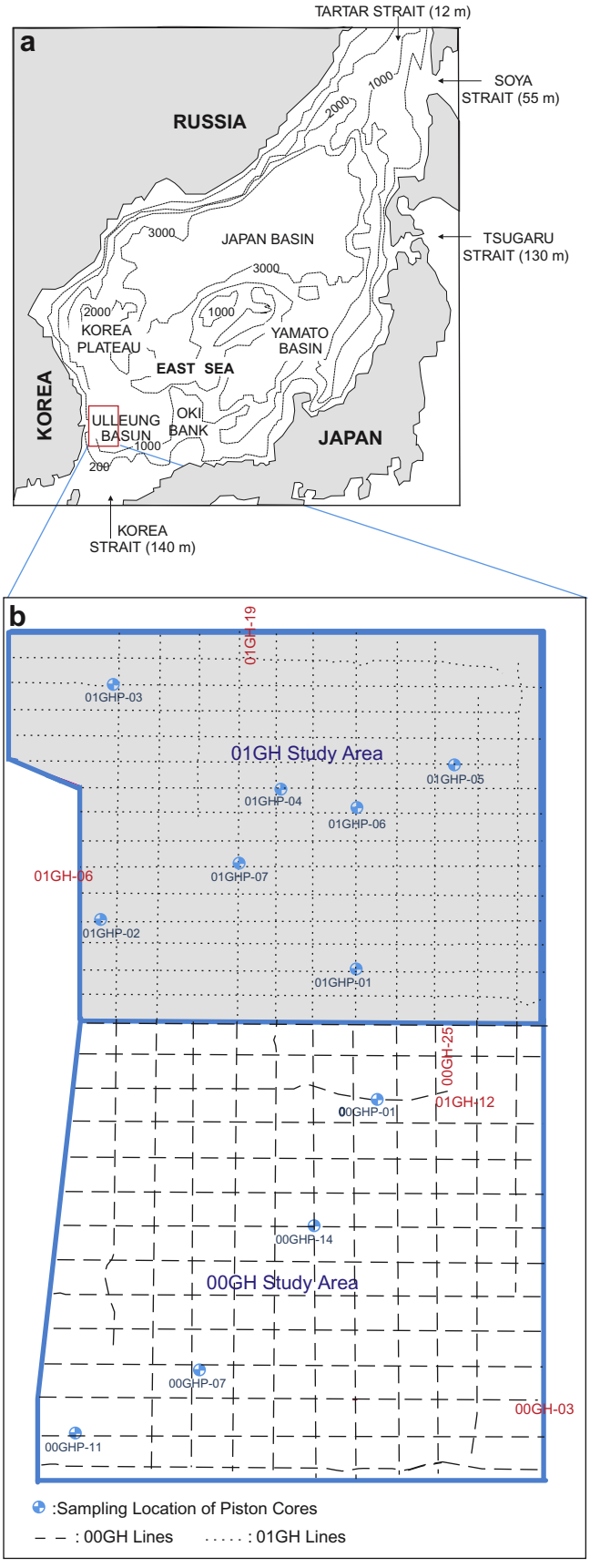

Fig. 1. (a) Physiographic map of the East Sea and the surrounding region (bathymetry in meters). Box indicates study area expanded in (b). (b) Seismic lines and location of piston cores in 00GH and 01GH study areas.

Using the research vessel TAMHAE-2 of KIGAM, 4782 km of seismic lines and 23 piston cores 5–8 m in length were collected in the western Ulleung Basin. The regional data were analyzed by KIGAM with additional research processing of some seismic lines and other studies in a cooperative program with the Pacific Geoscience Centre (PGC), Geological Survey of Canada (GSC).

A number of geological (e.g., McIver, 1977, 1982; Kvenvolden, 1993; Kvenvolden and Lorenson, 2001), geochemical (e.g., Kastner et al., 1995; Sloan, 1998; Dählmann and De Lange, 2003) and geophysical (e.g., Shipley et al., 1979; White, 1979; Dillon et al., 1998; Hyndman et al., 2001) indicators are available to detect and quantify gas hydrate. Marine gas hydrates are stable in mid-latitude marine sediments only under the high pressure and low temperature conditions that occur beneath water depths generally greater than about 600 m. Therefore our study is only of the deeper water areas of the Ulleung Basin. Upward fluid movement that carries gas (mainly methane) is concluded to be a primary source of the gas contained within hydrate form as well as the associated underlying free gas (e.g., Hyndman and Davis, 1992; Haacke et al., 2008). Bottom-simulating reflectors (BSRs) are commonly associated with marine gas hydrate systems and reflect the trapping of free gas below gas hydrate-bearing sediments. BSRs tend to be best developed where fluid migration is less focused, but occurs pervasively over larger regions. In contrast, more focused fluid movements can produce localized vent or upwelling structures that also commonly contain gas hydrate (e.g., Riedel et al., 2002; Trehu et al., 2004). We report evidence for the occurrence of gas hydrate in the Ulleung Basin that reflect both regional and focused modes of gas migration.

Although massive gas hydrate has been recovered by piston coring and drilling in a few places, it is most common, particularly where the hydrates are disseminated, for the hydrate to fully dissociate during recovery. However, where hydrate is not recovered, there are a number of indicators in cores for the presence of in-situ hydrate. Features such as bedding-parallel cracks and soupy ("moussey") textures were well observed in Northern Cascadia cores of ODP gas hydrate drilling Leg 146 (Westbrook et al., 1994; Kastner et al., 1995), and are considered indicators for dissociation of in-situ gas hydrates (Westbrook et al., 1994; Kastner et al., 1995; Kvenvolden and Lorenson, 2001). Cracks formed by gas expansion were also seen in Cascadia cores of ODP Leg 204 (Riedel et al., 2006a), and both cracks and soupy textures were observed in cores from the Ulleung Basin, (Ryu et al., 2005). Other indicators of in-situ gas hydrate that has dissociated upon recovery are cold core temperatures immediately upon recovery (e.g., Long et al., 2003; Trehu et al., 2004; Su et al., 2006; Riedel et al., 2006b), and low pore fluid chlorinities (e.g., Whiticar et al., 1995; Paull et al., 2000b; Tomaru et al., 2006).

The bottom-simulating reflector (BSR) is the most commonly used geophysical indicator of marine gas hydrates, and are often used to provide an initial indication of potential gas hydrate distribution. BSRs occur at the interface between overlying hydrate-bearing sediments and underlying gas-bearing sediments with lower velocity. However, BSRs provide limited information on the concentrations and thicknesses of hydrate or free gas (e.g., Fujii et al., 2008). BSRs are generally nearly parallel to the sea floor following an isotherm. BSR sub-bottom depths increase with increasing water depth, following the pressure–temperature phase stability of hydrate. Local BSR-depth variations usually indicate local variations in heat flow (e.g., Hyndman et al., 1993). They are often characterized by large reflection coefficients and reflection polarity opposite to that of the seafloor reflection (Shipley et al., 1979; Hyndman and Spence, 1992; Paull et al., 1997).

Vertical to sub-vertical seismic blanking zones of reduced reflectivity are one of the more recently recognized indicators of gas hydrate (e.g., Riedel et al., 2002). Only a few of these

structures have been studied in detail, but blanking zones are often associated with cold fluid and gas vents characterized by extensive seafloor carbonate formations and cold-vent chemosynthetic communities. A number of hydrate samples were retrieved from blanking zones by piston coring and deep-drilling on the Cascadia margin (Solem et al., 2002; Riedel et al., 2002, 2006b) and the Ulleung Basin region of our study (NETL, 2007; Park et al., 2008).

In this study, 11 piston cores from the western deep-water Ulleung Basin (Fig. 1) were analyzed to investigate the 1) origins of the methane and organic matter in the sediments, 2) the potential of hydrocarbon gas generation in the upper few hundred meters of sediments and 3) the potential for near-seafloor hydrate. In addition, 4782 km of 2D multi-channel seismic lines were analyzed to find indicators of gas hydrates and to estimate their distribution (Fig. 1).

2. Regional setting

The study area is in the western Ulleung Basin, in the southwestern East Sea off the east coast of Korea (Fig. 1). The East Sea is a semi-closed marginal sea between the Eurasian continent and the Japan Arc. It is connected with open oceans through 12–140 m deep straits (e.g., Moriyasu, 1972) and is composed of three deep oceanic sedimentary basins, Ulleung, Yamato, and Japan Basins. They are separated by submarine topographic highs including the Korea Plateau, Yamato Ridge, and the Oki Bank that rise to within about 500 m of the sea surface (Fig. 1).

The continental shelf on the west side of the basin is narrow and flanked by very steep slopes, whereas the shelves on the south and east are broad and flanked by rather gentle slopes. The basin floor gradually deepens to the north and northeast from 1000 m to 2300 m. There are a few seamounts formed by volcanic activity in the northeastern part of the basin. The basin is connected northward to the Japan Basin through the Korea Gap (e.g., Park, 2007), a long narrow interplain gap (Fig. 1), between Ulleungdo and Dokdo islands.

The Ulleung Basin was formed during Late Oligocene to Early Miocene by crustal extension associated with southward drift of the Japan Arc away from the Asian mainland (Tamaki et al., 1992; Jolivet et al., 1995; Chough and Barg, 1987). At the end of the Middle Miocene (ca. 12 Ma), the tectonic regime changed from tensional to compressional (Yoon and Chough, 1995; Chough et al., 2000). This led to thrust faulting and folding in the southern and western margin of the basin and to the sediment compression and consolidation that probably has been responsible for the upward flow of gas-rich fluids and hydrate formation. Since the end of Late Miocene, the basin has progressively subsided until the present (Park et al., 2002).

According to earlier seismic studies, Chough et al. (2000) divided the sediment section into four seismic sequence units. The lowermost is a Late Oligocene – Early Miocene unit of volcanic flows and sills intercalated with sedimentary layers. This is overlain by a Middle Miocene marine shale unit that is uniform in thickness in the central basin and grades to the northeast into a unit that is characterized by massive sandstone/shale, volcaniclastics and turbidite sequences. Third is a thick Late Miocene – Early Pliocene marine shale unit that is interbedded with thin sandstone and siltstone beds. The grain size and associated permeability contrasts may provide important controls on gas hydrate formation. In the southern part of the basin, this Early Pliocene unit is characterized by slide or slump deposits. The uppermost unit consists of Late Pliocene – Quaternary turbidites and hemipelagic muds and/or mass-flow deposits.

3. Material and methods

3.1. Core sampling and analyses

Eleven 5–8 m piston cores were analyzed in this study (00GHP: 4 cores, 01GHP: 7 cores; see Fig. 1 for location). The cores were taken in water depths ranging from 790 m to 2 174 m. The cores were kept in the cold sample storage of R/V TAMHAE-2 at 4 °C under constant humidity conditions immediately after their recovery and transported to the sample storage at the KIGAM laboratory using a refrigerator car.

The cores were analyzed for (1) sedimentary textures and facies, (2) total organic carbon (TOC) and nitrogen (N), (3) the origin, composition and concentration of residual hydrocarbon gases, and (4) the depth of the sulfate–methane interface (SMI). In the laboratory, the cores were split and one half preserved as an archive and the other half processed as a working core. X-ray radiographs of 1 cm thick slabs were taken to analyze the sedimentary textures and facies (aging time: 40 s, voltage for aging: 70 kVp, tube current: 3 mA).

A total of 822 samples were selected for Rock-Eval pyrolysis and elemental analyses at 5–10 cm intervals from 9 cores (4 of 00GHP cores, 5 of 01GHP cores: 01GHP-01 through 01GHP-04 and 01GHP-06; Fig. 1). The samples were freeze-dried and ground to homogenized powders for further analyses. TOC contents of the sediments were measured using the Rock-Eval pyrolysis technique that has often been used for the evaluation of the hydrocarbon source-rock potential of sedimentary rocks (e.g., Tissot and Welte, 1984; Peters, 1986). *N* was also measured to determine TOC/*N* ratios, which are commonly used to determine the depositional environments of the organic matter (e.g., Stein, 1991). Elemental and Rock-Eval pyrolysis analyses were performed using a LECO CHN-600 and a VINCI Rock-Eval-6 at KIGAM. For this study, we additionally refer to the analytical results of TOC and *N* for cores 01GHP-05 and 01GHP-07 by Park et al. (2005).

The concentrations of residual hydrocarbon gases in the core sediments were analyzed using the headspace technique. For the cores collected prior to publication of ODP Technical Note 30 by Pimmel and Claypool (2001), our 16 samples were taken from the 8 cores onboard after recovery and immediately placed with seawater into sealed cans as was the common procedure on hydrocarbon exploration drill ships. For the cores retrieved in 2002 (01GHP-05 through 01GHP-07; Fig. 1), two 5-cm^3 samples were taken from each core onboard after recovery and immediately placed into the 20-cm^3 vial as described by Pimmel and Claypool (2001). In 2002, the samples were analyzed by both using a sealed can and using a vial for comparison. There was no significant difference in the residual hydrocarbon gas results for the different sampling techniques.

In the KIGAM laboratory, gas extracted through the septum was injected with a glass syringe into a Hewlett Packard HP 5890 II gas chromatograph (GC). The amounts of headspace gases were calculated using sample weight, total weight, sample volume, space volume, sediment volume, and pore water volume. Carbon isotopic compositions ($\delta^{13}C$) of the residual hydrocarbon gases were determined using isotope ratio mass spectrometry (IRMS) at the Korea Research Institute of Standard and Science (KRISS) using the same samples used for headspace gas analysis. The IRMS consists of a Hewlett Packard HP 6890 GC and a Finnigan MAT GC Combustion III, with analytical reproducibility of $\pm 0.4‰$.

The concentrations of sulfate (SO_4^{2-}) were analyzed to measure sulfate–methane interface (SMI) depths, which are used to estimate the upward methane fluxes (e.g., Borowski et al., 1996). Sulfate was analyzed using pore water extracted from the two piston cores from the 00GHP study area as described by Gieskes et al. (1991) and

immediately placed into the glass vial as described by Pimmel and Claypool (2001). These additional cores were collected from the same sites of the cores 00GHP-07 and 00GHP-14. The pore water was extracted from core samples by centrifuging for 30 min at 10 000 rpm and collected with a syringe and filtered using 0.45-μm membrane filters. Sulfate was analyzed using Dionex ion chromatography (DX-500 IC) with an AS-40 autosampler at the Seoul National University in Korea. The SMI of cores of the 01GHP study area was measured using the sulfate concentrations analyzed by Park et al. (2005).

3.2. Seismic data acquisition and processing

A total of 4782 km (2511 km for 00GH lines and 2271 km for 01GH lines) of 2D multi-channel reflection seismic data were acquired in the western Ulleung Basin in 2000 and 2001. For the 00GH lines the seismic source volumes were mainly 4.9 l (299 in^3), the streamer consisted of 96 channels, and shot and group intervals were 12.5 m and 6.25 m respectively. For the 01GH lines the source volumes were 15.1 l (925 in^3) and 20.5 l (1254 in^3), the streamer consisted of 80 channels, and the shot and group intervals 25 m and 12.5 m respectively (Table 1). The active array lengths and maximum offsets were limited by heavy fishing activity to 600 m and 650 m for 00GH lines, and 1000 m and 1050 m for 01GH lines (Table 1). The array lengths are short for the water depth, which limited the interval velocity resolution, and restricted special processing that requires far offset data. The sample interval for digital recording was 1 ms. Systematic processing of the seismic data was conducted at KIGAM using the SUN Fire-3800 and LANDMARK ProMax2D processing systems and special processing analyses at the Pacific Geoscience Centre, Geological Survey of Canada using the Globe Claritas system from the Institute of Geological and Nuclear Sciences, New Zealand. Some initial results were presented by Lee et al. (2005).

The recorded data had strong low-frequency noise and several linear events, probably due to the effects of streamer motions that were removed in processing. The systematic processing of the data included: geometry definition and CMP sorting, 1st bandpass filter (minimum phase, 10-250 Hz), signature deconvolution (estimated from seafloor reflection), gap deconvolution (200 ms filter length, 10 ms gap), 2nd bandpass filter (minimum phase, 10–250 Hz), normal moveout correction (no stretch mute), semblance velocity analysis (selected regions with focus on BSR), and stack (full offset range).

The observed BSRs were characterized by (a) polarity opposite to that of the seafloor, (b) nearly seafloor-parallel reflection at sub-bottom depth corresponding to the expected base of the gas hydrate stability zone (BGHS) as determined from regional heat flow and thermal modeling, and (c) marked change in velocity, with distinctly lower values below the BSR. These features are consistent with the BSR being produced by free gas accumulations trapped by gas hydrates at the BGHS. The reflection coefficient of the BSR (RC_{BSR}) is useful for the estimation of the associated impedance and velocity contrasts, which provide some qualitative constraint on the amounts of hydrate and free gas (e.g., Fink and Spence, 1999;

Table 1
Acquisition parameters of 2D multi-channel seismic data analyzed for this study.

Seismic line		Source volume [liter (in^3)]	Shot interval [m]	Group interval [m]	No. of channel	Maximum offset [m]	Sample interval [ms]
00GH	00GH-05	7.4 (454)	12.5	6.25	96	650	1
	00GH-26A	4.0 (245)					
	00GH-22	10.4 (635)					
	00GH-23	17.0 (1035)					
	Other 00GH lines	4.9 (299)					
01GH	01GH-18 01GH-20 01GH-22 01GH-24 & 01GH-26	12.4 (754) 20.5 (1254)	25	12.5	80	1050	1
	Other 01GH lines	15.1 (925)	12.5	6.25			

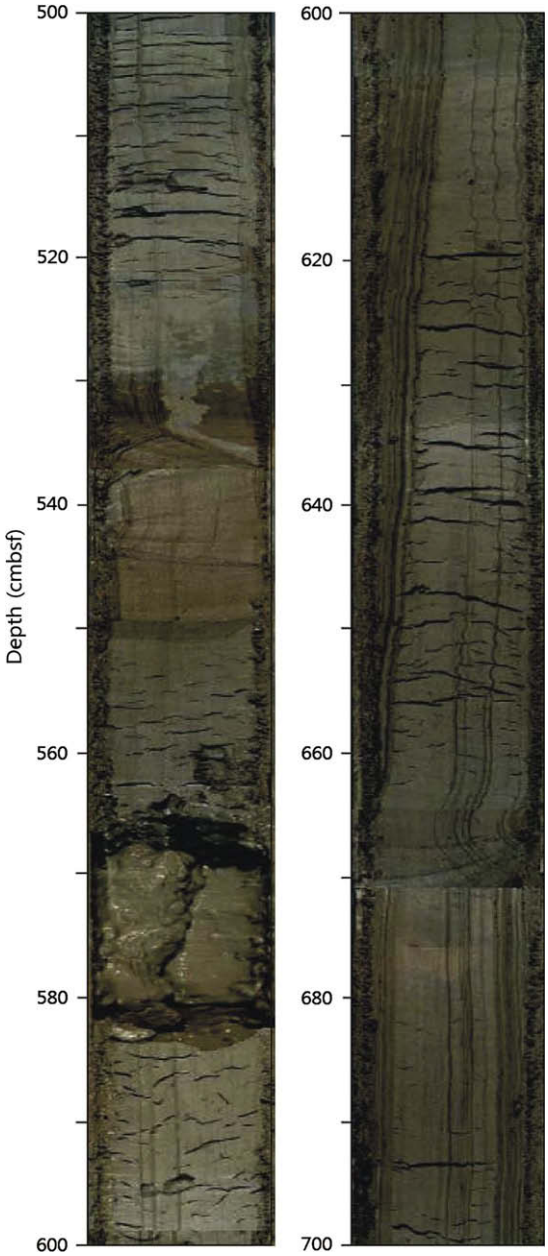

Fig. 2. Typical sediment textures with gas expansion cracks in recovered piston cores from the Ulleung Basin. Left panel: Core 00GHP-07; Right panel: core 00GHP-11.

Yuan et al., 1999). The reflection coefficient of the seafloor (RC_{sf}) was first estimated using the Warner (1990) seafloor multiple method:

$$RC_{sf} = 2A_{mult}/A_{prim} \quad (1)$$

where A_{prim} is the primary seafloor reflection coefficient and A_{mult} is the amplitude of the seafloor multiple. The RC_{BSR} was then calculated using:

$$RC_{BSR} = A_{BSR} \times F/\left(1 - RC_{sf}^2\right) \quad (2)$$

with the reflection amplitude of BSR (A_{BSR}) and conversion factor (F) estimated from the seafloor reflection coefficient study. No special provisions were made to preserve true amplitudes; however, the method uses amplitude ratios and the estimated BSR reflection coefficients are therefore believed not to be significantly biased by the processing.

The sedimentary layers in the study area are often bedded parallel to the seafloor so that the hydrate-related BSR may be hidden. Thus, seismic velocity analyses were an important tool to define the base of the hydrate stability zone. Velocity increase above or decrease below the BSR relative to a no-hydrate no-gas reference (as shown below) is also the primary tool to estimate the concentrations of hydrate and free gas.

An important requirement for estimating hydrate and free gas concentrations from velocity data is the no hydrate-no gas reference velocity-depth. As noted above, the short array lengths limit the accuracy of velocity estimates. However, the accuracy is sufficient for very useful hydrate and free gas concentration constraints. For the reference velocity-depth we have mainly interpolated the trend at depths well below the BSR and the velocities near the seafloor where we assume that there is little hydrate except in the blanking-vent structures. That there is little hydrate near the seafloor outside the blanking zones is supported by recent log velocity data in the area (Kim et al., 2008). This method can be used only if the sediment sections are reasonably homogeneous laterally and on a seismic wavelength scale vertically, with velocity increasing smoothly downward due to compaction. The reference velocity-depth was found to be quite constant for large regions of the study area and is given by:

$$V = 1510 + 0.5387T - 0.000085T^2 \quad (3)$$

with interval velocity V in m/s and T as two-way traveltime (TWT) in seconds below the seafloor. This velocity function is based on substantially more data including interval velocities, which should render it superior for estimation of gas hydrate concentration as compared to the function published in Lee et al. (2005); which relies solely on RMS velocities. Our regional velocity-depth relations are in general agreement with those from OBS refraction seismic experiments in the region (Kim et al., 1998). The velocities from OBS refraction studies for the upper few hundred meters of sediments range from 1500 m/s to 2300 m/s; however OBS velocities analyses are generally of lower spatial resolution than reflection seismic surveys. Significant deviations from this reference velocity-depth profile may be interpreted as due to high-velocity gas hydrate or low velocity underlying free gas, although lateral velocity variations due to lateral variations in sediment type and sediment consolidation cannot be excluded. The conversion to gas hydrate concentration from velocity increase relative to the reference velocity-depth, is discussed in a later section.

3.3. Thermal modeling and BSR depths

As mentioned above, the upper sediment section of the study area contains several strong reflectors at approximately the depth expected for the BGHSZ that in some cases show reversed polarity relative to the seafloor and are therefore interpreted to be BSRs driven by the transition from free gas to gas hydrate-bearing sediments. Unfortunately, the available marine heat flow probe data (Pollack et al., 1993; Yamano et al., 1996), and thus expected BSR depth, show large fluctuations over relatively short distances. Although much of the variability may be due to measurement uncertainty, seafloor temperature transients, and active seafloor sediment processes, the large variability in the data does not allow us to estimate the expected local BGHS depth accurately. Thus, thermal modeling was performed to predict the BGHS depth for several vertical temperature gradients around the preferred value based on the average of nearby thermal data. The seismic sections have been overlain by three isotherms representing gradients of 80 °C/km, 100 °C/km and 140 °C/km to indicate where the BGHSZ is expected to occur. The expected depth of the BSR (in ms TWT) was calculated using the gas hydrate stability function modified after Bouriak et al. (2000) for a seawater/methane mixture. Water depth is calculated from the seafloor traveltimes and converted to depth

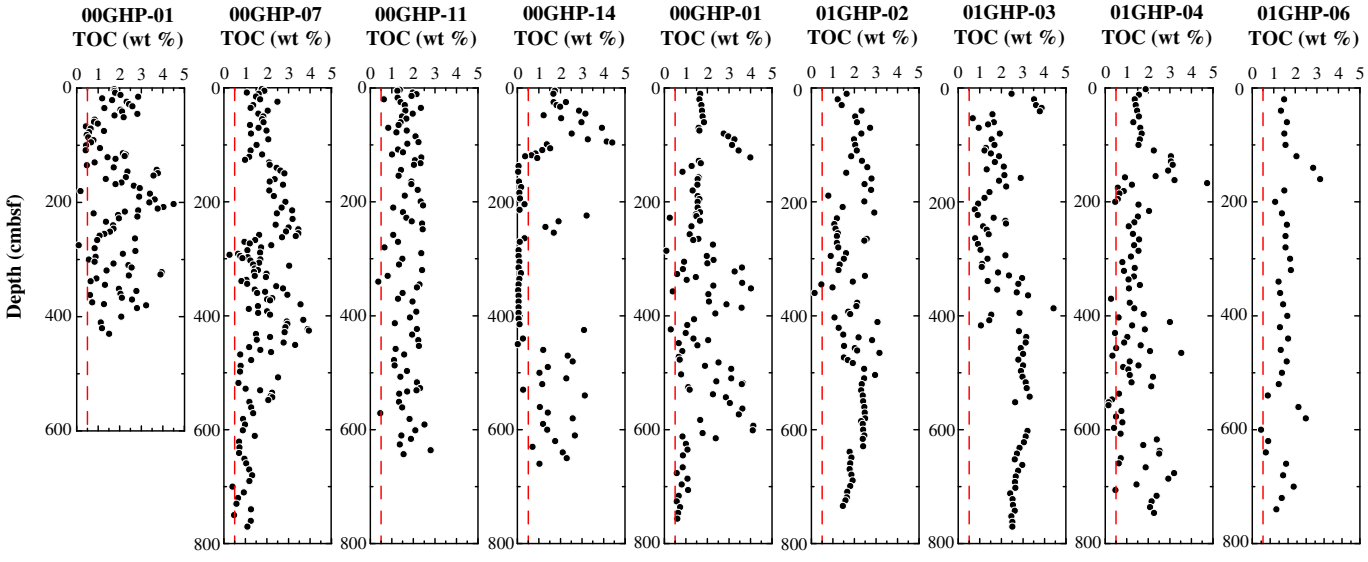

Fig. 3. TOC content of the core sediments as a function of depth.

using a constant water velocity of 1485 m/s from the seismic data average. Hydrostatic pressure is assumed at the BSR depth and pressure is calculated using a constant seawater density of 1030 kg/m^3. We follow the example of most previous estimates of heat flow from BSR depth that assumed hydrostatic pressure in the shallow sediments (Davis et al., 1990; Hyndman et al., 1993). We did not find a significant change in the calculated depth of the BSR for the range of velocities expected to represent the top ~200 mbsf (meter below seafloor) of sediments (1550–1600 m/s) in the Ulleung Basin. In all examples shown in this study, an average velocity above the BSR of 1550 m/s is used to calculate the isotherms.

Thermal conductivity is calculated using the empirically-defined relation by Davis et al. (1990) that relates thermal conductivity with velocity and depth. Although this relation was derived from an accretionary prism, the sediments are similar to those of the Ulleung Basin, i.e., deposited by turbidite currents and through general background pelagic sedimentation. There is also compressive deformation in both sediment sections. Future work is needed to measure thermal conductivity as a function of depth in the Ulleung Basin. The estimated thermal conductivity does not change significantly in the top ~200 mbsf. Seafloor temperatures were taken to vary with depth between 0 °C and 2 °C (Morita, 1984). These values agree well with those in the study area from expendable bathythermograph (XBT) water temperature profiles measured as part of this study.

3.4. Band-limited acoustic impedance inversion

In this analysis, we used a traveltime inversion approach to estimate band-limited impedance logs from stacked seismic data (e.g., Grevemeyer et al., 2000). The primary objective of this approach is to characterize the impedance contrast at the BSR, which can then be used to calculate the velocity contrast assuming that density does not vary significantly across the interface. The results are band-limited impedance-traveltime profiles, which remove most of the difficulties of waveform inversion such as interference artefacts and limited resolution in the analysis of the BSR reflection strength.

A good estimate of the wavelet is required for the inversion. Also, the amplitudes of the seismic data must be scaled to yield a reasonable seafloor reflection coefficient (~0.2). This scaling factor was also determined following the method by Warner (1990). Spherical divergence correction of the stacked seismic data is also applied.

This method is very robust for relative impedance changes; however the absolute values are uncertain if there is no prior knowledge of the background trend. The noise level (from data and numerically in the inversion computations) has a strong influence on the background trend; but a reference impedance-depth profile can be used (from density/velocity information) and the relative changes can then be projected on this general trend. Since we have used stacked data there could be an AVO effect; however, streamer offsets are small, the angle of incidence never exceeds 15 degrees, so no strong AVO effect is expected. Overall, this method is believed to give more reliable and detailed velocity changes across the BSR than using semblance-based interval velocities, especially as interval velocities are difficult to determine in the case of BSRs, where the RMS velocity reversal greatly complicates the use of the Dix (1955) equation for interval velocity calculation. Uncertainties in the picking of RMS velocities (mainly a result of a short streamer with small offsets) can result in negative (and thus meaningless) calculated interval velocities when using the Dix (1955) equation.

4. Results and discussion

4.1. Geological and geochemical indicators for gas hydrate and free gas

4.1.1. Core sedimentary textures

Gas hydrates contained in cored sediments are often largely dissociated by the pressure decrease and temperature increase that occurs during the recovery. When gas hydrate dissociates, it forms gas and nearly pure water that induce cracks and other disturbances in the textures of sediments and freshening of the pore water. Cracks generally developed parallel to the bedding were observed in the deeper intervals of the cores 00GHP-01, 00GHP-07 and 00GHP-11 (Fig. 2). Cracks also were observed in the lowermost interval of core 01GHP-01. The cracks are interpreted as formed by release of gas from the dissociation of gas hydrate. They also could be formed by expansion of in-situ free gas upon core recovery, but the in-situ conditions for the cores are within the stability zone of gas hydrate so free gas is not expected.

4.1.2. TOC content

Total Organic Carbon (TOC) is an important indicator of the potential for substantial hydrocarbon gas generation. In the 00GHP and 01GHP cores, contents of TOC ranged from 0.02% to 4.5% (average 1.7%) and from 0.1% to 4.7% (average 1.8%), respectively (Fig. 3). Most values are above 0.5% (93% of analyzed samples). Two intervals of core 00GHP-14 containing very low contents of TOC are mainly composed of coarser-grained sediments (sand- and gravel-sized). The sedimentation rates for cores 01GHP-04 and 01GHP-06 are 17 cm/kyr and 20 cm/kyr respectively (Park et al., 2006). These rates are higher than the minimum value suggested by Sloan (1998)

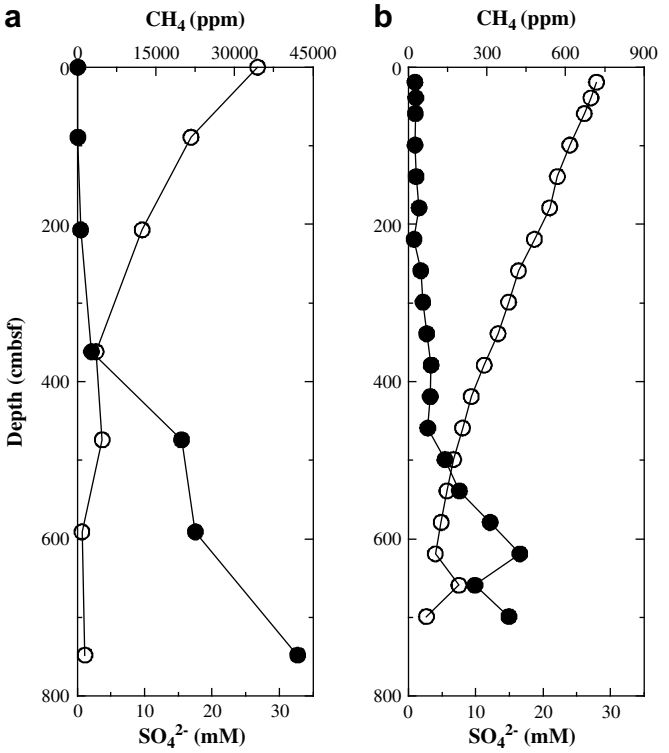

Fig. 4. Concentrations of sulfate in interstitial water and residual hydrocarbon gas in sediments of cores retrieved from the 00GH and 01GH study areas. (a): Core 00GHP-07; (b): core 01GHP-05. Open circle: Concentration of sulfate; Filled circle: concentration of residual hydrocarbon gas. The SMI in core 00GHP-07 is 350–400 cmbsf and about 600 cmbsf in core 01GHP-05.

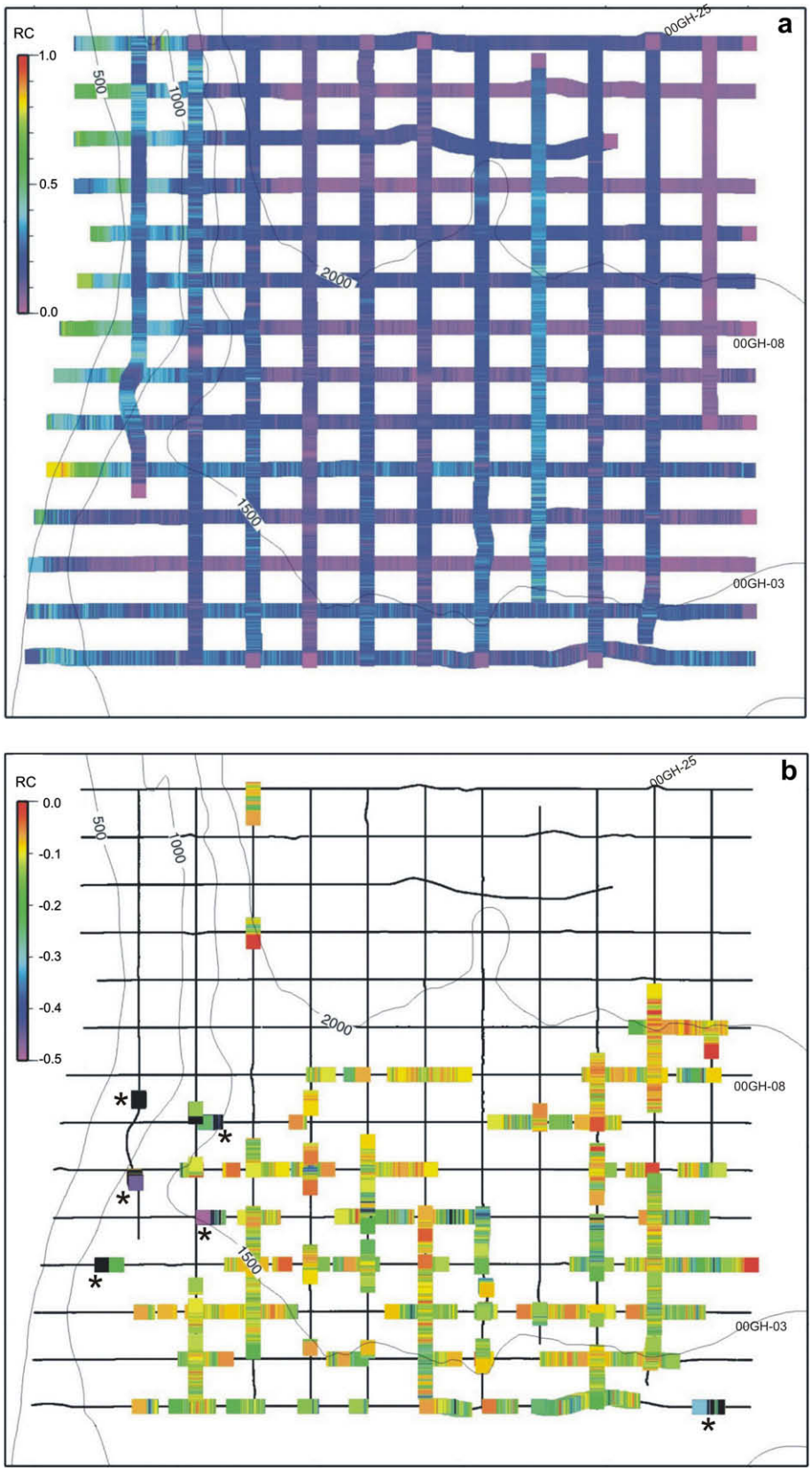

Fig. 5. Map of reflection coefficients from 00GH study area determined using Warner's (1990) method for (a) seafloor and (b) BSR. Locations annotated with a star showed very determined high reflection coefficients that are probably processing artefacts.

for significant organic diagenesis to occur. Moreover, the heat flow in the study area is high (Pollack et al., 1993; Yamano et al., 1996) as expected for a young backarc basin. The high sedimentation rate, organic carbon content and heat flow are favor the generation of substantial biogenic methane (e.g., Peters, 1986; Max et al., 1997; Sloan, 1998), which can form gas hydrates within the hydrate stability zone of the shallow sediments in the study area. If similar TOC content and sedimentation rate occur to considerable depth, then there is the potential for substantial amounts of biogenic methane and gas hydrate. Variations in the depth to the SMI data can suggest lateral differences in upward methane fluxes, and thus in potential methane content/generation at greater depth. However, this is only applicable if anaerobic methane oxidation is the dominant reaction responsible for sulfate reduction (Kastner et al., 2008).

TOC/*N* ratios can be used to characterize the type of organic matter in the sediments, because different groups of organisms produce sediment organic matter that contains different carbon and nitrogen contents. The TOC/*N* ratios of the core sediments are mostly from 4 to 12 indicating that the organic matter originated mainly from a marine source (e.g., Stein, 1991).

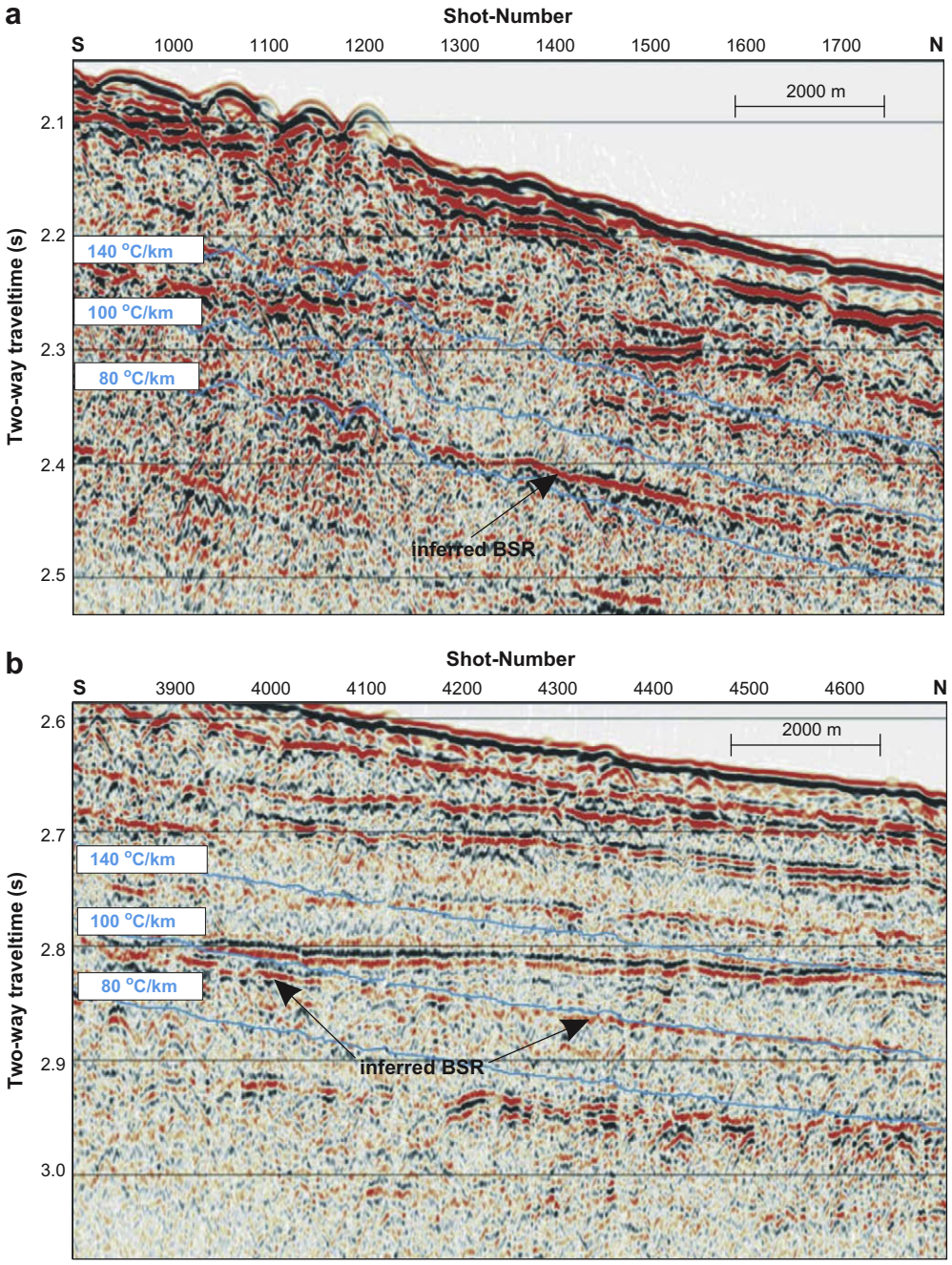

Fig. 6. Example of an inferred BSR occurrence in the Ulleung Basin from line 00GH-25. Note that BSR shallows northward in relation to the seafloor. (a) Southern part with BSR between the 80 °C/km and 100 °C/km isotherms and (b) northern section with BSR closer to the 100 °C/km isotherm. Note that the thermal model assumes constant physical properties along the line (velocity used is constant at 1550 m/s).

4.1.3. Residual hydrocarbon gas concentration

Although much of the in-situ gas is usually lost during core recovery, core headspace gas measurements can provide some qualitative information on variations of the in-situ concentration, and whether there is sufficient gas available for hydrate formation. The concentrations of hydrocarbon gases in the 00GHP and 01GHP cores varied between 0.13 and 87.4 ml/l (average 44 ml/l) of wet sediment, and between 0.04 and 35.4 ml/l (average 3.8 ml/l) of wet sediment, respectively (Table 2). Three among four 00GHP cores showed the residual hydrocarbon gas concentrations greater than the minimum value suggested by Sloan (1998) for the formation of significant gas hydrates. In contrast, in the 01GHP cores, concentrations of residual hydrocarbon gases are lower, excluding samples collected from the deeper intervals of cores 01GHP-01 and 01GHP-06 (Table 2). The cores having greater headspace gas concentrations correspond to those where there was strong disturbance of the sedimentary textures. This correspondence supports the conclusion that the sedimentary texture disturbance is caused by expansion of high concentrations of in-situ gas produced from hydrate upon recovery.

The variations in the concentration of residual hydrocarbon gases of the cores suggest regional differences in SMI depths and upward methane fluxes (e.g., Borowski et al., 1996). The SMI of core 00GHP-07 retrieved from the southern part of the 00GH study area would be situated at the depth between 350 cmbsf and 400 cmbsf (Fig. 4a). The interstitial water of core 00GHP-14 recovered from the middle part of the 00GH study area was concluded to be contaminated and resulted in artificially elevated sulfate values because this core contains high amounts of coarser sediments (sands and gravels) below 125 cmbsf. Thus, we were unable to define the SMI. The SMI depths of cores collected from the 01GHP study area determined on the basis of sulfate concentrations by Park et al. (2005) would be situated a little bit deeper. Results for core 01GHP-05 show that the SMI depth may be at near 600 cmbsf (Fig. 4b). When uncontaminated sulfate and methane profiles were obtained from the cores, they showed that the SMI is likely stretched over a zone up to several 10s of centimeters thick, which has also been seen in other areas e.g. off Vancouver Island during IODP Expedition 311 (Riedel et al., 2006b), and off India in the Krishna–Godavari basin during the NGHP Expedition 01 (Collett et al., 2008).

An important question for the source of gas for hydrate formation is whether the gas is biogenic or thermogenic. The residual hydrocarbon gases of our core sediments were mainly composed of methane (Table 2). Biogenic gas containing mainly methane is generally produced at relatively low temperatures and therefore shallow depth, whereas thermogenic gas containing higher hydrocarbons is produced mainly at higher temperatures and therefore greater depths (e.g., Tsunogai et al., 2002). The carbon isotopic composition of the methane ($\delta^{13}C_{CH4}$) was analyzed from the 00GHP cores. The core $\delta^{13}C_{CH4}$ values ranged from −78‰ to −75‰ again indicating that their origin is primarily biogenic (e.g., Sloan, 1998).

Table 2
Concentrations of residual hydrocarbon gases in the core sediments detected from head space gas analysis.

Core No.	Sample depth (cmbsf)	HC gas in sediment (ml/l of wet sediment)	C_1/total HC gas (Vol. %)	Sampling container
00GHP-01	113–118	59.63	99.8	Sealed can
	513–518	77.23	99.8	Sealed can
00GHP-07	395–400	37.49	99.9	Sealed can
	795–800	87.40	99.9	Sealed can
00GHP-11	395–400	39.26	100.0	Sealed can
	795–800	55.51	100.0	Sealed can
00GHP-14	395–400	0.13	100.0	Sealed can
	795–800	0.41	98.8	Sealed can
01GHP-01	365–370	0.22	97.8	Sealed can
	763–768	12.62	99.9	Sealed can
01GHP-02	367–372	0.04	99.9	Sealed can
	737–742	0.05	96.9	Sealed can
01GHP-03	372–377	0.10	95.0	Sealed can
	772–777	0.16	98.3	Sealed can
01GHP-04	362–367	0.07	95.7	Sealed can
	755–760	1.44	95.7	Sealed can
01GHP-05	356–361	0.42	100.0	Vial
	730–735	1.20	100.0	Vial
01GHP-06	353–358	0.41	100.0	Vial
	750–755	35.44	99.8	Vial
01GHP-07	324–329	0.43	100.0	Vial
	727–732	0.94	100.0	Vial

HC: hydrocarbon; C_1: methane.

4.2. Geophysical indicators of gas hydrate and free gas

4.2.1. BSR

4.2.1.1. General occurrence of hydrate BSRs. In our study area, BSRs were found in a number of local patches. Fig. 5 shows a map with seafloor and BSR reflection coefficients for the 00GH lines. As noted above, the seafloor reflection coefficient is used as a calibration in

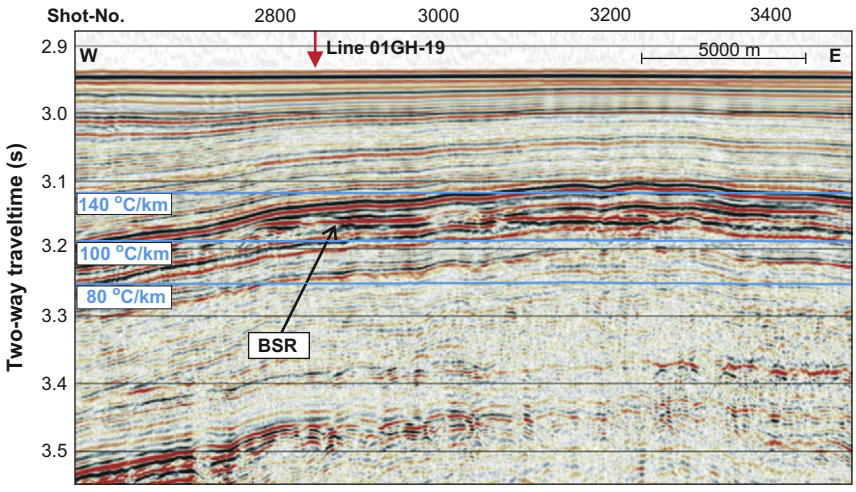

Fig. 7. Example of seismic section of line 01GH-06 showing the most extensive BSR occurrence in the 01GH study area.

calculating the BSR reflection coefficient. The seafloor reflection coefficient is mainly below 0.2, although there are higher values locally (Fig. 5a). The cause of the local high reflection coefficients could be a change in sedimentary composition or a complex interference pattern from several near surface sediment layers. Seafloor carbonates produced by oxidation of hydrocarbon gas expelled through the seafloor are also a possible explanation for high seafloor reflection coefficients. The very heterogeneous character of the BSR reflection amplitudes in combination with variable seafloor reflection amplitude diminishes the accuracy of the calculated BSR reflection coefficients. Seafloor reflection coefficients average 0.10 and the BSR averages about −0.04 (Fig. 5). As a comparison, BSR reflection coefficients of the study area are much lower than observed in a number of other areas, e.g., Cascadia offshore Vancouver Island, where a typical widespread BSR has a reflection coefficient around −0.1 (e.g. Yuan et al., 1999; Chapman et al., 2002), and the Beaufort Sea margin of about 0.06 (Andreassen et al., 1995) and Nankai Trough (e.g., Foucher et al., 2002). The BSR reflection coefficients suggest a velocity decrease of about 100 m/s assuming a constant density across the interface and background velocities (i.e. no gas hydrate) above the interface. However, many regions in the area of investigation show elevated reflection coefficients of up to −0.1, which corresponds to a velocity drop of ~300 m/s under the same assumptions as mentioned above. The simple use of reflection coefficients cannot resolve the question whether the reflection is due to overlying gas hydrate, underlying free gas or a combination thereof. In our calculations we simply assumed that the BSR is entirely due to free gas below the interface. If the reflection is solely due to overlying high-velocity hydrate, the concentration could be about 10% saturation, using the simple porosity reduction model (e.g., Hyndman and Spence, 1992). If the BSR reflection is solely due to underlying low-velocity free gas, the gas concentration required is lower than 1% if the gas is uniformly distributed throughout the sediment to a depth below the BSR of at

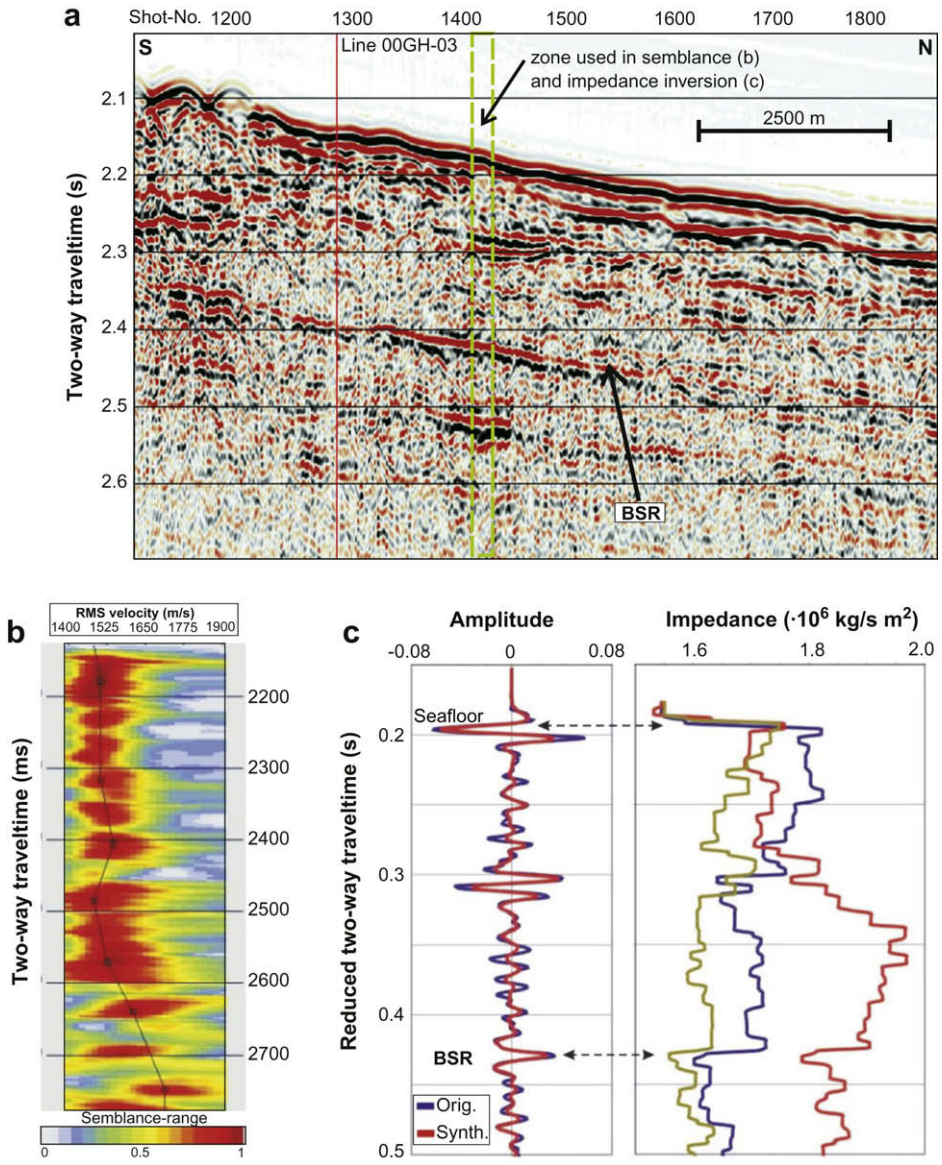

Fig. 8. (a) Example of a laterally continuous BSR in the Ulleung Basin from seismic line 00GH-25. (b) Detailed semblance velocity analyses show a decrease in RMS velocity of around 50 m/s at TWT of 2450 ms; however conversion to interval velocity using Dix (1955) is inaccurate. (c) Results of band-limited impedance inversion. A good match between original and synthetic seismic traces was found for the BSR reflection and the resulting impedance decrease amounts to a velocity decrease of maximum 100 m/s. Shown are three impedance profiles for the traces falling into the green box shown in (a).

least a seismic wavelength (~25 m). As shown by Chapman et al. (2002), the BSR reflection is strongly dependent on the seismic frequency and tuning effects can alter the reflection strengths significantly if the velocity transition is over a thickness similar to the seismic wavelength. This low concentration is unlikely to be mobile upward.

In order to detect the hydrate BSRs where they may be well developed but masked by the concordancy of the BGHS with stratigraphy, the depths for the expected base of the hydrate stability zone were estimated using temperature gradients based on the regional heat flow data as outlined above. The lateral variations in thermal conductivities and seismic velocities are concluded not to be significant. Three model BGHS depth contours representing a reasonable range of geothermal gradients were overlain on seismic sections to guide the identification of BSRs for comparison with high and low velocity intervals interpreted to result from hydrate and underlying free gas.

A south to north shallowing in BSR-depth relative to the seafloor has been observed in the 00GH study area (see also Horozal et al., 2008). Since the water depth increases northward, the pressure effect should result in the opposite trend, a deepening of the BSR for constant heat flow. Thermal modeling showed that in the southern area the interpreted BSR depths fit the 90 °C/km isotherm and in the central area fit the 100 °C/km isotherm or slightly above (Fig. 6), at least partially explaining the northward shallowing of the BSR. This trend may be explained by greater tectonic extension and therefore heat flow in the central part of the basin during its formation. These high thermal gradients (heat flow over 100 mW/m^2) are expected for this geologically young basin.

BSRs are present widely in the southeastern part of 00GH study area, but are localized and patchy. However, in 01GH study area, they occur only very locally in the midwestern and northeastern parts. An especially strong and laterally consistent BSR was also observed associated with a gentle anticlinal structure in the western part of the 01GH study area where seismic lines of 01GH-06 and 01GH-19 cross (Figs. 1 and 7). The BSR within the anticline may result from focusing of rising fluids carrying methane toward the center of the structure. No BSR could be identified on the steep slopes toward the western part of the study area.

4.2.1.2. Velocity decrease at BSR. Our primary method for estimating concentrations of gas hydrate and free gas from seismic data is based on velocity deviations from reference no-hydrate, no-gas velocity-depth profiles (equation (3) above). In this section we discuss velocity deviations from the reference described above, mainly for sediments above BSRs. The short hydrophone streamer offsets limited the accuracy of the interval velocities but some important velocity-depth trends were observed. In the 00GH study area, there is a general small downward increase of interval velocity with depth toward the BSR as expected due to normal sediment consolidation, but regionally no distinct increase in velocity above the BSR relative to the reference. The RMS velocity often decreases slightly below the BSR probably due to very small free gas concentration. On a few lines, the RMS velocities decrease beneath the BSR by up to 60 m/s relative to the reference profile suggesting significant free gas (Fig. 8a and b). We conclude that free gas below the BSR is localized and concentrations are generally low.

A part of line 00GH-25 between shot-numbers 1400 and 1450 showed a clear BSR and therefore was chosen for band-limited acoustic impedance inversion to further quantify the velocity decrease at the BSR (Fig. 8a and c). An overall good correlation between the computed synthetic and original data traces was found. The corresponding relative impedance profiles all show a clear drop of impedance at the BSR depth of around 140 000 kg/sm^2. In order to estimate the corresponding velocity decrease at this interface, we first assume that the density does not change

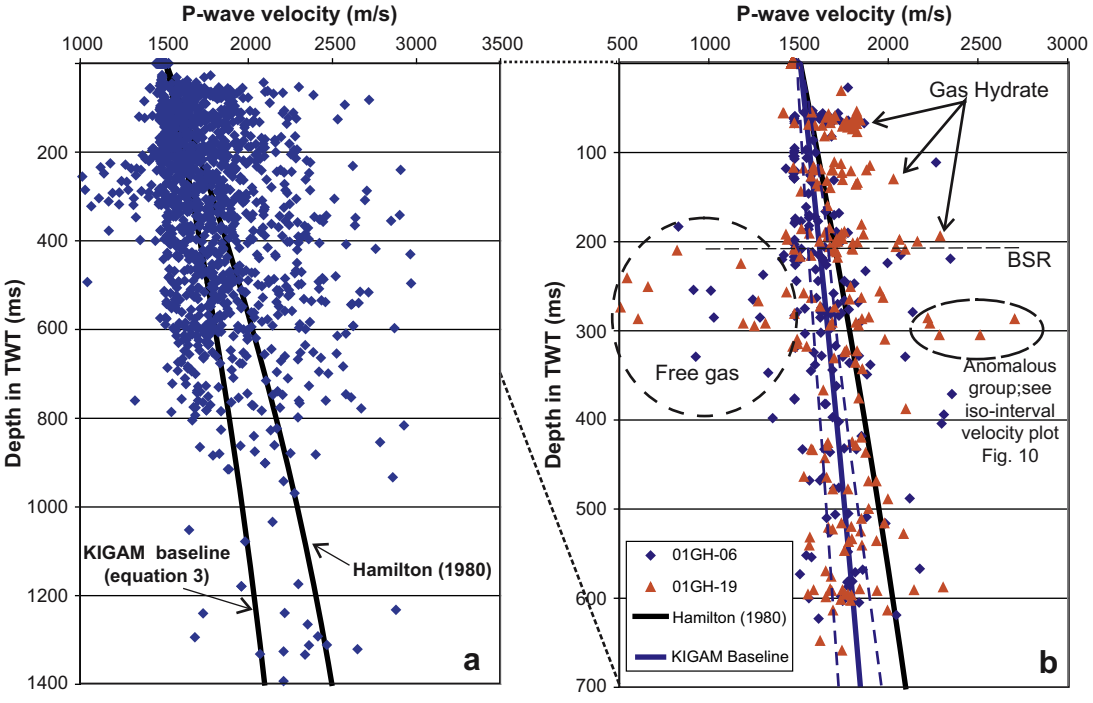

Fig. 9. (a) Results of all interval velocity values determined from the 00GH and 01GH study areas in comparison to the Hamilton (1980) velocity trend for shallow marine sediments and our KIGAM baseline for no gas/no gas hydrate (equation (3)). (b) Detailed analyses at the anticline structure in the 01GH study area reveal two distinct layers with substantially higher interval velocities than suggested by the KIGAM baseline. Also seen are lower values below the BSR. However, these values were determined with the Dix (1955) formula and are likely inaccurate. However, they suggest the presence of some free gas. The dashed lines represent an estimate of uncertainty (1 standard-deviation from maximum to minimum possible velocity). Also note the change in vertical scale in (b).

across the BSR. In the absence of deep-drilling data available, we secondly have to assume a specific density value to calculate the velocity from the impedance. Assuming a reasonable range of possible densities from 1500 kg/m^3 to 1850 kg/m^3 the above impedance contrast represents a velocity decrease between 80 m/s and 100 m/s, or 5–6%, respectively.

4.2.1.3. Anticlinal structure with strong BSR. The highest-amplitude and regionally extensive BSR occurs over the broad gentle anticline in the 01GH study area as noted above (Fig. 7). A series of special seismic analyses were performed to characterize the velocity field in that area. The interval velocities were determined using the Dix formula to about 200 ms TWT depth below the seafloor with reasonable accuracy above the BSR. For two reflectors above the BSR, the velocities are between 1750 m/s and 2000 m/s (Fig. 9). These velocities are much higher than our regional no-hydrate, no-gas reference (equation (3) above), suggesting that those layers are probably gas hydrate-bearing. For the two main reflectors at 40 and 140 ms TWT below the seafloor, the reference velocities are 1531 and 1584 m/s respectively. Using the simple porosity reduction model (e.g., Hyndman and Spence, 1992) and an empirical velocity–porosity relation based on the three-phase weighted equation by Lee et al. (1993), the estimated average gas hydrate concentrations are between 20% and 25% of pore space. The concentrations may be higher in thin layers within these intervals and there may be strong lateral variability. With the uncertainties in seismic velocities and in the conversion of velocity anomaly to hydrate concentration, these concentration estimates have considerable uncertainty,

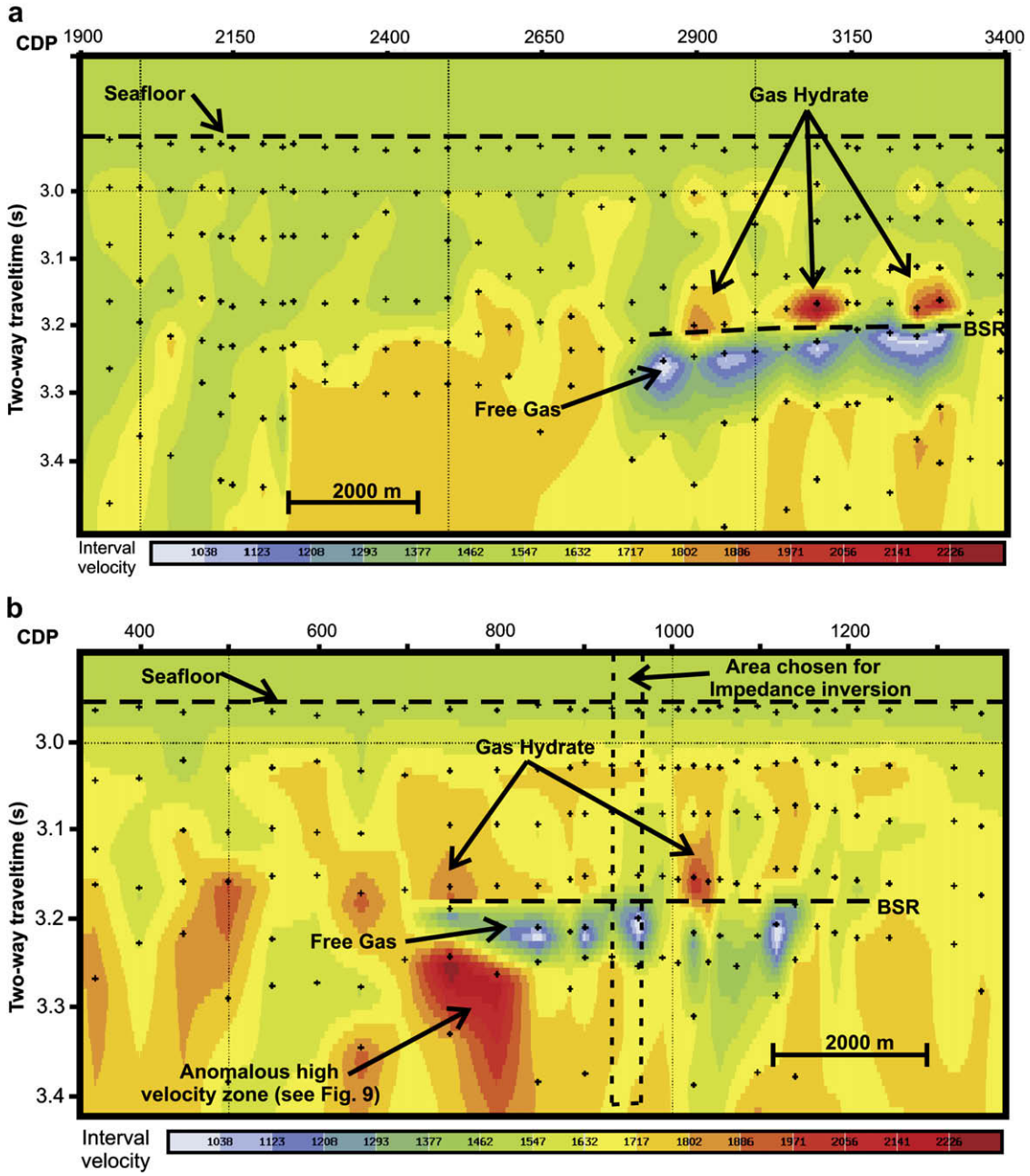

Fig. 10. Velocity contour images from anticline in the 01GH study area that has a strong BSR. Shown are results indicating low-velocity free gas underlying high-velocity hydrate, for (a) line 01GH-06 and (b) line 01GH-19. Compare to Fig. 7 for seismic images. Impedance inversion was performed on selected locations along line 01GH-19.

perhaps as much as 50%, but there is likely significant hydrate concentration over this broad region.

At several locations on both seismic lines there are substantially low interval velocities below the BSR indicative of free gas (Figs. 9 and 10). Interval velocities using the Dix formula can have substantial error where downward velocity decreases are encountered, such as below the BSR, and as noted above, the semblance-based velocity analysis has a considerable inaccuracy due to the short streamer offsets. However, the data are adequate to show conclusively that there is a low velocity layer below the BSR in this area. Longer hydrophone array lengths giving larger offsets are needed for higher accuracy velocities.

In order to further quantify the velocity change at the BSR, band-limited acoustic impedance inversion was carried out at several locations along seismic line 01GH-19 (Fig. 10). The relative impedance contrast at the BSR is consistently between 140 000 kg/sm^2 and 190 000 kg/sm^2. Assuming again a range of densities from 1500 kg/m^3 to 1850 kg/m^3, the calculated impedance contrasts then represents a velocity decrease between 75 m/s and 125 m/s (or 5–8%).

4.2.2. Seismic blanking zones and upwelling structures

A number of seismic blanking zones up to 2 km across were observed in the seismic data (e.g., Lee et al., 2005). They may represent fluid upwelling regions; elsewhere such structures have been found to contain substantial amounts of gas hydrate; for example, massive gas hydrate was recovered in piston cores and Integrated Ocean Drilling Program (IODP) Expedition 311 drill cores from the upper 50 m of such a structure off Western Canada (e.g., Riedel et al., 2002, 2006b). One typical example of a seismic section containing a blanking zone is shown in Fig. 11.

Most of the blanking zones occur where the reflection images indicate bedded sediments in the mid-eastern part of the study area. Some zones were also locally found in the northern part of the 01GH study area. Only a few blanking zones were found in the southern portion of 00GH study area where widespread BSRs were

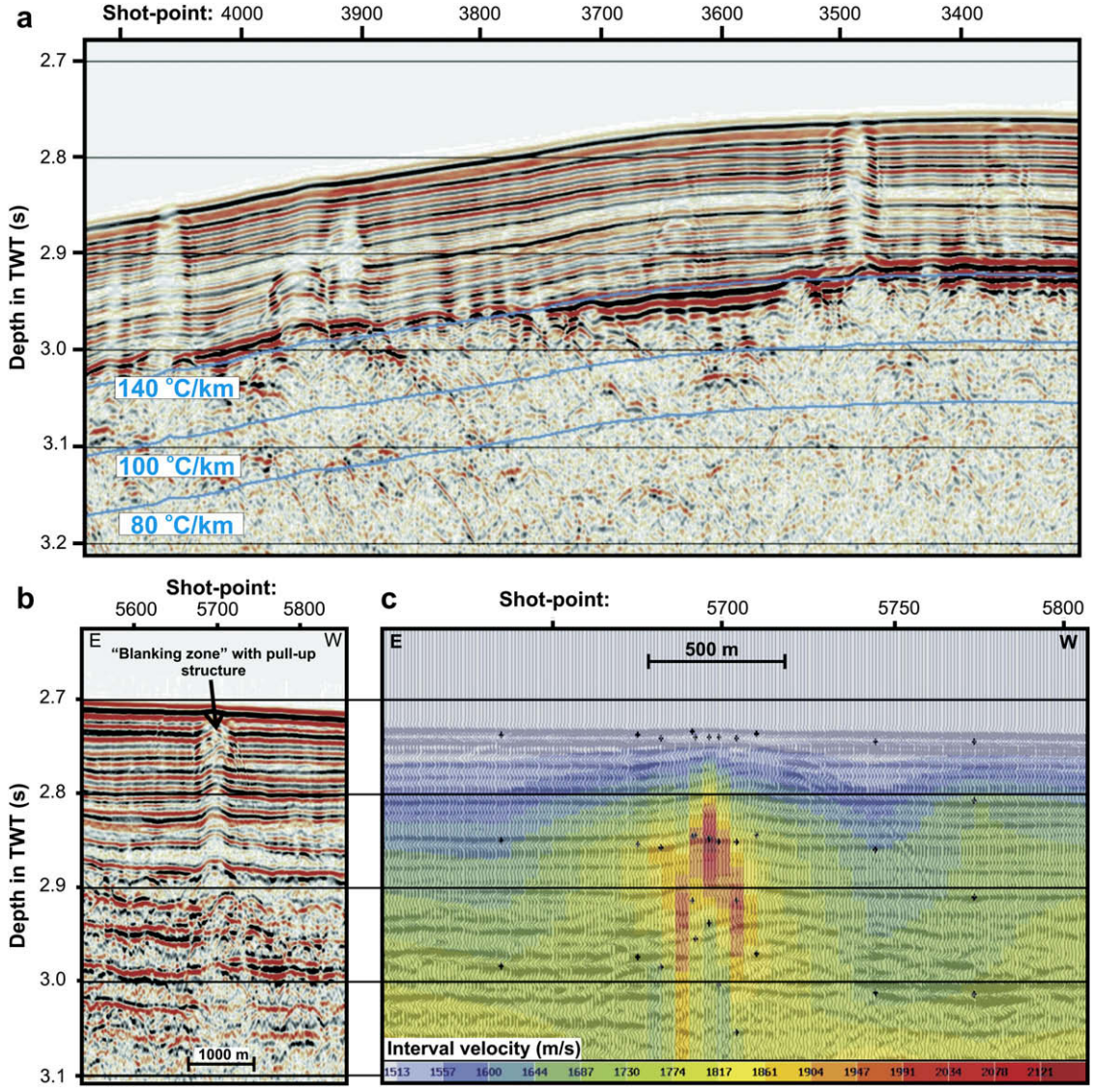

Fig. 11. (a) Example of several blanking zone structures in the 00GH study area (along seismic line 00GH-13). (b) Example of a blanking zone in the 00GH study area (along seismic line 00GH-10, see also Lee et al., 2005) with apparent velocity pull-up interpreted to be at least partly due to high-velocity hydrate. (c) A close-up of the area around the features with the seismic traces underlain by interval velocity from semblance analyses. Inside the blanking zones, velocities are significantly increased to over 2000 m/s relative to the sediments outside of the blanking zone, which typically show values around 1600–1700 m/s.

identified. The difference in inferred fluid flux from local vents to broad upwelling that produces BSRs may reflect differences in regional sediment permeability associated with changes in geologic heterogeneity, both stratigraphic and deformational. No blanking zones were found on the steeper continental slope in the western part of the study areas.

The blanking zones are near-vertical broad structures of reduced reflectivity compared to adjacent sediments, up to 300 ms TWT thick (about 200 m) and commonly rest on a thick sequence of acoustically transparent sediments. Although they appear as "chimneys" in the commonly vertically exaggerated seismic sections, they actually usually are wider than high. Many of the blanking zones have bowing up of sediment bedding reflectors in time sections that may result mainly from high-velocity hydrate, i.e., velocity pull-up (near-horizontal sediment reflectors that extend through the structure are warped upward) (Lee et al., 2005). High interval velocities from some of these structures support this interpretation.

Detailed velocity analysis of pre-stack CDP gathers across one blanking zone with an apparent pull-up structure in the 00GH study area showed strongly increased interval velocities in the blanking zone (Fig. 11). The high velocities are located mainly in the centre of the blank zone but the horizontal resolution is too low to resolve the velocity variation across the structure. The seismic data were processed using Dip-Move-Out (DMO) to reduce the influence of structural dip in the velocity determination. We interpret the observed high interval velocities inside the blanking zone as evidence for the presence of gas hydrate, confirming the earlier initial calculations reported by Lee et al. (2005), that did not include detailed semblance-based velocity analyses. Recent near-seafloor gas hydrate discoveries from some of these blanking zones in 2007 support our interpretation (NETL, 2007; Park, 2008; Kim et al., 2008; Park et al., 2008).

5. Conclusions

The seismic surveys, piston coring, and other studies of marine gas hydrate in the western deep-water Ulleung Basin of the East Sea off the east coast of Korea have given the following results:

1. Geological and geochemical data derived from study of piston cores support the interpretation of gas hydrate occurrence in the area. In the cores, there are cracks generally developed parallel to the bedding that are interpreted to be caused by the expansion on recovery of substantial gas produced by dissociation of in-situ hydrate. The core analyses showed high amounts of total organic carbon (TOC) and high core headspace gas that indicate favorable conditions for gas hydrate formation in shallow sediments. The lack of higher hydrocarbons and the $\delta^{13}C_{CH4}$ ratios indicate that the methane is primarily biogenic. The SMI depths of cores retrieved from the northern study area are deeper than that of core recovered from the southern study area, suggesting higher methane fluxes in the southern study area.
2. Clear bottom-simulating reflectors (BSRs) are not widespread but have been mapped in several areas of the western Ulleung Basin. These BSRs are interpreted to be a caused by free gas trapped by gas hydrate at the BHGS based on, (a) reversed reflection polarity, (b) seafloor-parallel reflection, especially cross-cutting stratigraphic reflectors, and (c) located at sub-bottom depth corresponding to the expected base of the stability zone, as determined by thermal modeling of regional heat flow data. The systematic seismic surveys have mapped several areas with patchy BSRs, mainly in the southeastern portion of the study area. No BSRs were identified on the steep slopes toward the western part of the study area. Most of the reflectors are weak and probably represent only small concentrations of gas hydrate and/or underlying free gas. However, high-amplitude BSRs were observed in a few areas, especially over a gentle anticlinal structure in the 01GH study area. Vertical incidence reflection coefficients of the BSR average −0.15 at the anticline structure, representing a velocity contrast of about 400 m/s assuming a constant density across the BSR and no gas hydrate accumulation in the layer just above the BSAR, i.e. a background velocity of 1630 m/s. There is also higher than normal velocity within two layers at shallower depth (40 and 140 ms TWT, respectively) that suggests moderate concentration gas hydrate within the anticline.
3. Velocity analyses were used to define a regional no-hydrate, no-gas velocity-depth profile that is reasonably constant across the main part of the western Ulleung Basin. Increased velocities above some BSRs suggest hydrate concentrations; the higher-amplitude BSRs also are commonly associated with downward velocity decrease indicating underlying free gas. Velocity analyses over the regional BSRs suggest usually only small concentrations of gas hydrate, but the hydrate concentrations for the anticlinal structure in the 01GH study area are estimated to be a maximum average of 25% of pore space. A distinct decrease in seismic RMS and interval velocities just beneath the BSR at the anticline structure also indicates the presence of free gas.
4. A number of large seismic blanking zones up to 2 km across were observed in the western Ulleung Basin. In these structures the seismic stratigraphic reflectivity is much reduced. They often are associated with apparent velocity pull-up in time sections that we conclude is primarily due to enhanced seismic velocities, based on high interval velocities. They therefore may contain the highest concentrations of gas hydrate within the study area. However, large uncertainties remain in the gas hydrate concentration estimates due to (1) limitations in the seismic velocity analyses, (2) due to the uncertainty in the general applicability of the no-hydrate reference velocity profile, and (3) due to uncertainties in the relation between the velocity increase and hydrate concentration.

Acknowledgements

This research was supported by the Basic Research Project of Korea Institute of Geoscience and Mineral Resources (KIGAM) funded by the Ministry of Commerce, Industry and Energy (now Ministry of Knowledge Economy) and Korea Gas Corporation. We sincerely thank the scientists and technical staffs working as a part of this gas hydrate study at KIGAM and GSC-PGC, and the crew of R/V TAMHAE-2 responsible for the data and sample collection. Geological Survey of Canada publication number ESS#2005520.

References

Andreassen, K., Hart, P.E., Grantz, A., 1995. Seismic studies of a bottom simulating reflection related to gas hydrate beneath the continental margin of the Beaufort Sea. J. Geophy. Res. 100, 12659–12673.

Borowski, W.S., Paull, C.K., Ussler, W.I.I.I., 1996. Marine pore water sulfate profiles indicate in situ methane flux from underlying gas hydrate. Geology 24, 655–658.

Bouriak, S., Vanneste, M., Saoutkine, A., 2000. Inferred gas hydrates and clay diapers near the Storegga Slide on the southern edge of the Voring Plateau, offshore Norway. Mar. Geol. 163, 125–148.

Chapman, N.R., Gettrust, J., Walia, R., Hannay, D., Spence, G.D., Wood, W., Hyndman, R.D., 2002. High resolution deep-towed multichannel seismic survey of deep sea gas hydrates off western Canada. Geophysics 67, 1038–1047.

Chough, S.K., Barg, E., 1987. Tectonic history of the Ulleung Basin margin, East Sea (Sea of Japan). Geology 15, 45–48.

Chough, S.K., Lee, H.J., Yoon, S.H., 2000. Marine Geology of Korean Seas, second ed. Elsvier, Amsterdam, 313 pp.
Collett, T., Riedel, M., Cochran, J., Boswell, R., Presley, J., Kumar, P., Sathe, A., Sethi, A., Lall, M., Siball, V., the NGHP Expedition 01 Scientific Party, 2008. Indian National Gas Hydrate Program Expedition 01 Initial Reports: Prepared by the United States Geological Survey. The Directorate General of Hydrocarbons, Ministry of Petroleum and Natural Gas, India.
Dählmann, A., De Lange, G.J., 2003. Fluid-sediment interactions at Eastern Mediterranean mud volcanoes: a stable isotope study from ODP Leg 160. Earth Planet Sci. Lett. 212, 377–391.
Davis, E.E., Hyndman, R.D., Villinger, H., 1990. Rates of fluid expulsion across the northern Cascadia accretionary prism: constraints from new heat flow and multichannel seismic reflection data. J. Geophys. Res. 95, 8869–8889.
Dillon, W.P., Danforth, W.W., Hutchinson, D.R., Drury, R.M., Taylor, M.H., Booth, J.S., 1998. Evidence for faulting related to dissociation of gas hydrate and release of methane off the southeastern United States. In: Henriet, J.P., Mienert, J. (Eds.), Gas Hydrates-Relevance to World Margin Stability and Climate Change. Geol. Soc. Special Publ, vol. 137. Geol. Soc. Publishing House, London, pp. 293–302.
Dix, C.H., 1955. Seismic velocities from surface measurements. Geophysics 20, 68–86.
Fink, C.R., Spence, G.D., 1999. Hydrate distribution off Vancouver Island from multifrequency single-channel seismic reflection data. J. Geophys. Res. 104, 2909–2922.
Foucher, J.-P., Nouse, H., Henry, P., 2002. Observation and tentative interpretation of a double BSR on the Nankai slope. Mar. Geol. 187, 161–175.
Fujii, T., Saeki, T., Kobayashi, T., Inamori, T., Hayashi, M., Takano, O., Takayama, T., Kawasaki, T., Nagakubo, S., Nakamizu M., Yokoi, K., 2008. Resource assessment of methane hydrate in the eastern Nankai Trough, Japan. In: 6th International Conference on Gas Hydrates (ICGH 2008), Vancouver 2008, p. 68 (also 12 pp. in CD).
Gardner, J.M., Shor, A.N., Jung, W.Y., 1998. Acoustic imagery evidence for methane hydrates in the Ulleung Basin. Mar. Geophys. Res. 20, 495–503.
Grevemeyer, I., Rosenberger, A., Villinger, H., 2000. Natural gas hydrates on the continental slope off Pakistan: constraints from seismic techniques. Geophys. J. Int. 140, 295–310.
Gieskes, J.M., Gamo, T., Brumsack, H., 1991. Chemical methods for interstitial water analysis aboard JOIDES Resolution. ODP Tech. Note, 15. Ocean Drilling Program, College Station, TX, 60 pp.
Haacke, R.R., Park, K.P., Stoian, I., Hyndman, R.D., Schmidt, U., 2008. High-flux gas venting in the East Sea, Korea, from analysis of 2D seismic reflection data. In: 6th International Conference on Gas Hydrates (ICGH 2008), Vancouver 2008, p. 97 (also 9 pp. in CD).
Hamilton, E.L., 1980. Geoacoustic modeling of the seafloor. J. Acoust. Soc. Am., 68, 1313–1340.
Haq, B.U., 2000. Climate impact of natural gas hydrate. In: Max, M.D. (Ed.), Natural Gas Hydrate in Oceanic and Permafrost Environments. Kluwer Academic Publishers, Dordrecht, pp. 137–148.
Horozal, S., Lee, G.H., Yoo, D.G., Park, K.-P., Lee, H.Y., Kim, H.J., 2008. Seismic indicators of gas hydrate and associated gas in the Ulleung Basin, East Sea (Japan Sea) and implications of heat flow derived from depths of the bottom-simulating reflector. Marine Geology, 258, 126–138.
Hyndman, R.D., Davis, E.E., 1992. A mechanism for the formation of methane hydrate and seafloor bottom-simulating reflectors by vertical fluid expulsion. J. Geophys. Res. 97, 7025–7041.
Hyndman, R.D., Spence, G.D., 1992. A seismic study of methane hydrate bottom simulating reflectors. J. Geophys. Res. 97, 6683–6698.
Hyndman, R.D., Wang, K., Yuan, T., Spence, G.D., 1993. Tectonic sediment thickening: fluid expulsion and the thermal regime of subduction zone accretionary prisms: the Cascadia Margin off Vancouver Island. J. Geophys. Res. 98, 21865–21876.
Hyndman, R.D., Spence, G.D., Chapman, R., Riedel, M., Edwards, R.N., 2001. Geophysical studies of marine gas hydrate in northern Cascadia. In: Paull, C.K., Dillon, W.P. (Eds.), Natural Gas Hydrates Occurrence, Distribution, and Detection. Geophys. Monogr, vol. 124. AGU, Washington, pp. 273–295.
Jolivet, L., Shibuya, H., Fournier, M., 1995. Paleomagnetc rotation and the Japan Sea opening. In: Taylor, B., Natland, J. (Eds.), Active Margin and Marginal Basins of the Western Pacifics. Geophys. Monogr, vol. 88. AGU, Washington, pp. 358–369.
Kastner, M., Kvenvolden, K.A., Whiticar, M.J., Camerlenghi, A., Lorenson, T.D., 1995. Relation between pore fluid chemistry and gas hydrate associated with bottom-simulating reflectors at the Cascadia Margin, Site 889 and 892. In: Crason, B., Westbrook, G.K., Musgrave, R.J., Suess, E. (Eds.), Proc. ODP, Sci. Results, vol. 146. Ocean Drilling Program, College Station, TX, pp. 175–187 (Pt. 1).
Kastner, M., Torres, M., Solomon, E., Spivack, A.J., 2008. Marine pore fluid profiles of dissolved sulfate; do they reflect in situ methane fluxes? In: Fire in the Ice, NETL Methane Hydrate Newsletter, Summer 2008. Available online at: http://netl.doe.gov/scngo/Natural%Gas/hydrates/, pp. 6–8.
Kim, H.-J., Han, S.-J., Lee, G.H., Huh, S., 1998. Seismic study of the Ulleung Basin crust and its implications for the opening of the East Sea (Japan Sea). Mar. Geophys. Res. 20, 219–237.
Kim, G.Y., Yoo, D.G., Kim, W.S., Lee, H.Y., Park, K.P., 2008. Physical properties of gas hydrate-bearing sediments in the Ulleung Basin, the east sea of Korea: preliminary result from well-log data. In: 6th International Conference on Gas Hydrates (ICGH 2008), Vancouver 2008, p. 118 (also 4 pp. in CD).
Kvenvolden, K.A., 1993. Gas hydrates – geological prospective and global change. Rev. Geophys. 31, 173–187.
Kvenvolden, K.A., Lorenson, T.D., 2001. The global occurrence of natural gas hydrate. In: Paull, C.K., Dillon, W.P. (Eds.), Natural Gas Hydrates, Occurrence, Distribution, and Detection. Geophys. Monogr, vol. 124. AGU, Washington, pp. 3–18.
Lee, M.W., Hutchinson, D.R., Collett, T.S., Dillon, W.P., 1993. Seismic velocities for hydrate-bearing sediments using weighted equation. J. Geophys. Res. 101, 20347–20358.
Lee, J.H., Baek, Y.S., Ryu, B.J., Riedel, M., Hyndman, R.D., 2005. A seismic survey to detect natural gas hydrate in the East Sea of Korea. Mar. Geophys. Res. 26, 51–59.
Long, P.E., Riedel, M., Truhe, A.M., Collett, T., Weinberger, J., Torresd, M., Rack, F., Bohrman, G., Shipboard Scientific Party, Leg 204, 2003. Abundance and texture of gas hydrate beneath Hydrate Ridge, Offshore Oregon, USA from infrared imaging. In: EGS-AGU-EUG Joint Assembly, Nice 2003, vol. 5, 07999.
MacDonald, G.T., 1990. Role of methane clathrates in past and future climates. Climate Change 16, 247–281.
Max, M.D., Pellanbarg, R.E., Hurdle, B.G., 1997. Methane hydrates, a special clathrate: its attributes and potential. U.S. NRL Rept. NRL/MR/6101-97-7926, NRL, Washington, 74 pp.
McIver, R.D., 1977. Role of natural gas-important agent in geological process. Geol. Soc. Am. Abst. Prog. 9, 1089–1090.
McIver, R.D., 1982. Role of naturally occurring gas hydrates in sediment transport. AAPG Bull. 66, 789–792.
Morita, Y., 1984. Paleoenvironment of the Sea of Japan. In: Oertu, H.J. (Ed.), BENTHOS '83: Second International Symposium on Benthic Foraminifera, Pau 1983. Elf Aquitaine, Pau, pp. 409–414.
Moriyasu, S., 1972. The tsushima current. In: Stommel, H., Yoshida, K. (Eds.), Kuroshio, Its Physical Aspects. Univ. of Tokyo Press, Tokyo, pp. 353–369.
NETL, 2007. Early results from Korean gas hydrate research effort are encouraging. In: Fire in the Ice, NETL Methane Hydrate Newsletter, Fall 2007. Available online at: http://netl.doe.gov/scngo/Natural%Gas/hydrates/, p. 12.
Park, C.H., 2007. Hydrography of the East Sea. In: Lee, K.-S., Kim, W.-S. (Eds.), Ocean Atlas of Korea – East Sea. National Oceanographic Research Institute, Incheon, pp. 66–75.
Park, K.P., 2008. Gas hydrate exploration activities in Korea. In: 6th International Conference on Gas Hydrates (ICGH 2008), Vancouver 2008, p. 62 (also 7 pp. in CD).
Park, S.J., Yoon, S.H., Chough, S.K., 2002. Evolution of sedimentary basin in the SW Ulleung Basin margin East Sea (Sea of Japan). In: Korea–Japan Symposium – Possible Collaboration on East Sea (Sea of Japan) Scientific Drilling between Korea and Japan in Relation to Integrated Ocean Drilling Program (IODP), Gyeongju, pp. 83–99.
Park, M.H., Kim, J.H., Kim, I.S., Ryu, B.J., 2005. Tephrostratigraphy and paleo-environmental implications of Late Quaternary sediments and interstitial water in the western Ulleung, Basin, East Sea. Geo. Mar. Lett. 25, 54–62.
Park, M.-H., Kim, J.-H., Ryu, B.-J., Kim, I.-S., Chang, H.-W., 2006. AMS radiocarbon dating of the marine late Pleistocene–Holocene sediment cores from the western Ulleung Basin, East/Japan Sea. Nucl. Instrum. Methods Phys. Res. B Beam Interact. Mater. Atoms 243, 211–215.
Park, K.-P., Bahk, J.-J., Kwon, Y., Kim, G.Y., Riedel, M., Holland, M., Schultheiss, P., Rose, K., the UBGH-1 scientific party, 2008. Korean national program expedition confirms rich gas hydrate deposit in the Ulleung Basin, East Sea. In: Fire in the Ice, NETL Methane Hydrate Newsletter, Spring 2008. Available online at: http://netl.doe.gov/scngo/Natural%Gas/hydrates/, pp. 6–9.
Paull, C.K., Matsumoto, R., Wallace, P.J., et al., 1997. Proc. ODP, Init. Repts, vol. 164. Ocean Drilling Program, College Station, TX, 623 pp.
Paull, C.K., Ussler III, W., Dillon, W.P., 2000a. Potential role of gas hydrate decomposition in generating submarine slope failures. In: Max, M.D. (Ed.), Natural Gas Hydrate in Oceanic and Permafrost Environments. Kluwer Academic Publishers, Dordrecht, pp. 149–156.
Paull, C.K., Lorenson, T.D., Borowski, W.S., Ussler III, W., Olsen, K., Rodriguez, N.M., Wehner, H., 2000b. Isotopic composition of CH_4, CO_2 species, and sedimentary organic matter within ODP Leg 164 sample from Blake Ridge: gas source implications. In: Paull, C.K., Matsumoto, R., Wallace, P.J., Dillon, W.P. (Eds.), Proc. ODP, Sci. Results, vol. 164. Ocean Drilling Program, College Station, TX, pp. 67–78.
Peters, K.E., 1986. Guideline for evaluating petroleum source rock using programmed pyrolysis. AAPG Bull. 70, 318–329.
Pimmel, A., Claypool, G., 2001. Introduction to shipboard organic geochemistry on the JOIDES resolution. ODP Tech. Note, 30. Ocean Drilling Program, College Station, TX, 29 pp.
Pollack, H.N., Hunter, S.J., Johnson, J.R., 1993. Heat flow from the Earth's interior: analysis of the global data set. Rev. Geophys. 31, 267–280.
Riedel, M., Hyndman, R.D., Spence, G.D., Chapman, R., 2002. Seismic investigations of an apparent active vent field associated with gas hydrates, offshore Vancouver Island. J. Geophys. Res. 107, 5-1–5-16.
Riedel, M., Long, P., Liu, C.S., Schultheiss, P., Collett, T., ODP Leg 204 Shipboard Scientific Party, 2006a. Physical properties of near-surface sediments at Southern Hydrate Ridge: results from ODP Leg 204. In: Trehu, A.M., Bohrman, G., Torres, M.E., Colwell, F.S. (Eds.), Proc. ODP, Sci. Results, vol. 204. Ocean Drilling Program, College Station, TX.
Riedel, M., Collett, T.S., Malone, M.J., the Expedition 311 Scientists, 2006b. Proc. IODP, vol. 311. Integrated Ocean Drilling Program Management International, Inc., Washington, DC, doi:10.2204/iodp.proc.311.2006.
Ryu, B.-J., Lee, Y.-J., Kim, J.-H., Kim, I.-S., Park, M.-H., 2005. Geological and geochemical indicators for natural gas hydrates in shallow sediments of the western Ulleung Basin, East Sea. In: International Symposium on Gas Hydrate Technology, Seoul 2005, pp. 38–44.

Shipley, T.H., Houston, M.H., Buffler, R.T., Shaub, F.J., McMillen, K.J., Ladd, J.W., Worzel, J.L., 1979. Seismic reflection evidence for the widespread occurrence of possible gas-hydrate horizons on continental slopes and rises. AAPG Bull. 63, 2204–2213.

Sloan, E.D., 1998. Clathrate Hydrates of Natural Gases, second ed. Marcel Dekker, New York. 705pp.

Solem, R.C., Spence, G.D., Vukajlovich, D., Hyndman, R.D., Riedel, M., Novosel, I., Kastner, M., 2002. Methane advection and gas hydrate formation within an active vent field offshore Vancouver Island. In: 4th International Conference on Gas Hydrates, Yokohama 2002, pp. 84–89.

Stein, R., 1991. Accumulation of Organic Carbon in Marine Sediments. Springer, Berlin. 217pp.

Su, X., Song, C.-B., Fang, N.-Q., 2006. Relationship between sediment granulometry and the presence of gas hydrate on Hydrate Ridge. In: Trehu, A.M., Bohrman, G., Torres, M.E., Colwell, F.S. (Eds.), Proc. ODP, Sci. Results, vol. 164. Ocean Drilling Program, College Station, TX.

Tamaki, K., Suyehiro, K., Allan, J., Ingle Jr., J.C., Pisciotto, K.A., 1992. Tectonic synthesis and implications of Japan Sea ODP drilling. In: Tamaki, K., Suyehiro, K., Allen, J., McWilliams, M. (Eds.), Proc. ODP, Sci. Results, vol. 127/128. Ocean Drilling Program, College Station, TX, pp. 1333–1348 (Pt. 2).

Tissot, B., Welte, D.H., 1984. Petroleum Formation and Occurrence. Springer, Berlin. 538pp.

Tomaru, H., Matsumoto, R., Torres, M.E., Borowski, W.S., 2006. Geological and geochemical constraints on the isotopic composition of interstitial waters from the Hydrate Ridge region, Cascadia continental margin. In: Trehu, A.M., Bohrman, G., Torres, M.E., Colwell, F.S. (Eds.), Proc. ODP, Sci. Results, vol. 164. Ocean Drilling Program, College Station, TX.

Trehu, A.M., Long, P.E., Torres, M.E., et al., 2004. Three dimensional distribution of gas hydrate beneath southern Hydrate Ridge: constraints from ODP Leg 204. Earth Planet. Sci. Lett. 222, 845–862.

Tsunogai, U., Yoshida, N., Gamo, T., 2002. Carbon isotopic evidence of methane oxidation through sulfate reduction in sediment beneath cold seep vents on the seafloor at Nankai Trough. Mar. Geol. 187, 145–160.

Warner, M., 1990. Absolute reflection coefficients from deep seismic reflections. Tectonophys. 173, 15–23.

Westbrook, G.K., Carson, B., Musgrave, R.J., et al., 1994. Proc. ODP, Init. Repts, vol. 146. Ocean Drilling Program, College Station, TX (Pt. 1)611pp.

White, R.S., 1979. Gas hydrate layers trapping free gas in the Gulf of Oman. Earth Planet. Sci. Lett. 42, 114–120.

Whiticar, M.J., Hovland, M., Kastner, M., Sample, J.C., 1995. Organic geochemistry of gases, fluids, and hydrates at the Cascadia accretionary margin. In: Crason, B., Westbrook, G.K., Musgrave, R.J., Suess, E. (Eds.), Proc. ODP, Sci. Results, vol. 146. Ocean Drilling Program, College Station, TX, pp. 385–397 (Pt. 1).

Yamano, M., Shevaldin, Yu.V., Zimin, P.S., Baladashin, V.I., 1996. Heat flow in Japan Sea. In: Isezaki, N., Bersenv, I.I., Tamaki, K., Karp, B. Ya., Lelikov, E.P. (Eds.), Geology and Geophysics of the Japan Sea. Terra Sci. Publ., Japan–USSR Monogr. Ser, vol. 1, pp. 61–74.

Yoon, S.H., Chough, S.K., 1995. Regional strike slip in the eastern continental margin of Korea and its tectonic implications for the evolution of Ulleung Basin, East Sea (Sea of Japan). GSA Bull. 107, 83–97.

Yuan, T., Spence, G.D., Hyndman, R.D., Minshull, T.A., Singh, S.C., 1999. Seismic velocity studies of a gas hydrate bottom-simulating reflector on the northern Cascadia continental margin: amplitude modeling and full waveform inversion. J. Geophys. Res. 104, 1179–1191.